Computers and Concrete, *Vol. 17, No. 6 (2016) 723-737*
DOI: http://dx.doi.org/10.12989/cac.2016.17.6.723

The effect of non-persistent joints on sliding direction of rock slopes

Vahab Sarfarazi[1], Hadi Haeri[*2] and Alireza Khaloo[3]

[1]*Department of Mining Engineering, Hamedan University of Technology, Hamedan, Iran*
[2]*Department of Mining Engineering, Bafgh Branch, Islamic Azad University, Bafgh, Iran*
[3]*Center of Excellence in Structure and Earthquake Engineering, Sharif University of Technology, Tehran, Iran*

(Received February 10, 2016, Revised Feburary 28, 2016, Accepted February 29, 2016)

Abstract. In this paper an approach was described for determination of direction of sliding block in rock slopes containing planar non-persistent open joints. For this study, several gypsum blocks containing planar non-persistent open joints with dimensions of 15×15×15 cm were build. The rock bridges occupy 45, 90 and 135 cm^2 of total shear surface (225cm^2), and their configuration in shear plane were different. From each model, two similar blocks were prepared and were subjected to shearing under normal stresses of 3.33 and 7.77 kg/cm^{-2}. Based on the change in the configuration of rock-bridges, a factor called the Effective Joint Coefficient (EJC) was formulated, that is the ratio of the effective joint surface that is in front of the rock-bridge and the total shear surface. In general, the failure pattern is influenced by the EJC while shear strength is closely related to the failure pattern. It is observed that the propagation of wing tensile cracks or shear cracks depends on the EJC and the coalescence of wing cracks or shear cracks dominates the eventual failure pattern and determines the peak shear load of the rock specimens. So the EJC is a key factor to determine the sliding direction in rock slopes containing planar non-persistent open joints.

Keywords: planar non-persistent discontinuity; rock bridge; effective joint coefficient; tensile and shear cracks

1. Introduction

Predicting the stability of rock slopes is a classical problem for geotechnical engineers and also plays an important role when designing for dams, roads, tunnels and other engineering structures. The stability of the rock slopes is related to factors such as slope height, topographical dip, discontinuity plane angle, the engineering properties of the rock joints and rock bridges, the overburden weight, presence of water and other acting forces. One of the most important discussions in rock slopes stability is determination of moving direction of sliding block containing planar non persistent joint sets with similar dip angle (α in Fig. 1). In fact, predicting the moving direction of unstable block is useful for safe construction of the artificial structures

[*]Corresponding author, Assistant Professor, E-mail: haerihadi@gmail.com

http://www.techno-press.org/?journal=cac&subpage=8 ISSN: 1598-8198 (Print), 1598-818X (Online)

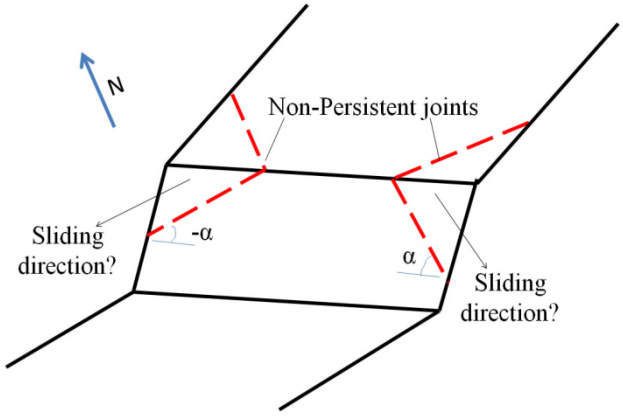

Fig. 1 The rock slope containing planar non-persistent open joints

around the rock slopes. To determine the moving direction in such a rock slopes, its important to know that the rock bridges in which direction have lower strength. Many studies have been carried out to determine the stability in rock slopes (Grenon and Hadjigeorgiou 2008, Singh *et al*. 2008, Duzgun and Bhasin 2009, Li *et al*. 2009, Li *et al*. 2009, Taheri and Tani 2010, Pantelidis 2011, Naghadehi *et al*. 2011, Gischig *et al*. 2011, Regmi *et al*. 2013, Sharma *et al*. 2013, Akin 2013, Zhao *et al*. 2015, Haeri 2015a, 2015b, Haeri and Sarfarazi 2016a, Haeri and Marji 2016b, Gao *et al*. 2016).

Terzaghi (1962), Robertson (1970), Einstein *et al*. (1983) suggest that the persistence of key discontinuity sets are in reality more limited and a complex interaction is needed in between the existing natural discontinuities and brittle fracture propagation through intact rock bridges to bring the slope to failure. So, besides the discontinuities themselves, the rock bridges, are of utmost importance for the shear strength of the compound failure plane (Jaeger 1971, Einstein *et al*. 1983). Different procedures can be used to study the strength of rock masses with non-persistent joints such as; field observations (as in the Hoek and Brown failure criterion); analytical solutions (as in Jenning's criterion); numerical studies (using available commercial software), or laboratory tests. Laboratory tests are an attractive procedure because they can expose failure mechanisms that may be complicated by other means. Laboratory tests are also useful to calibrate analytical solutions and numerical studies. Some previous results obtained with different test arrangements are summarized in the following paragraphs. Lajtai (1969) performed direct shear tests on model material with non-persistent joints and observed that the failure mode changed with increasing normal stress; he suggested a composite failure envelope to describe the transition from the tensile strength of the intact material to the residual strength of the discontinuities. He thus recognized that maximum shear strength develops only if the strength of the solid material and the joints are mobilized simultaneously. Other investigators conducted further experimental research to understand, in a qualitative way, the beginning, propagation and coalescence phenomena between two and three joints (Reyes and Einstein 1991, Shen *et al*. 1996, Mughieda and Khawaldeh 2004, Mughieda and Alzoubi 2004, Li *et al*. 2005, Mughieda and Khawaldeh 2006). Gehle & Kutter's (2003) investigation on the breakage and shear behavior of intermittent rock joints under direct shear loading condition showed that joint orientation is an important influential parameter for shear strength of jointed rock. Ghazvinian *et al*. (2007) made a thorough analysis of the shear behavior of the rock-bridges based on the change in the persistence of their area. The analysis

proved/showed that the failure mode and mechanism are under the effect of the continuity of the rock-bridge. In this paper, the effect of the configuration of the rock-bridges on the shear resistance of the non-persistent open joints is studied. By using this pilot study, the moving direction of sliding mass described in Fig. 1 is determined.

2. Experimental studies

The discussion of experimental studies is divided into four sections. The first section discusses the physical properties of a modelling material, the second section is describing the technique of preparing the jointed specimens, the third section is focused on the testing procedure in loading the jointed specimens and finally, the fourth section considers the general experimental observations and discussions.

Modelling material and its physical properties: Full scale testing on a rock mass containing a specified number of joints with predetermined configuration is seldom possible. The common procedure to the problem is to conduct experiments under conditions that are attainable, but the patterns of discontinuities involved in the prototype have to be preserved in the model experiments and the modelling material must behave similar to rock mass. The most comprehensive review on how to select a modelling material for rocks is probably by Stimpson (1970). There are a number of modelling materials that can be considered as rock-like material (Nelson and Hirschfeld 1968, Momber and Kovacevic 1997). The material used for this investigation is gypsum, the same material was used by Reyes and Einstein (1991), Takeuchi (1991), Shen *et al*. (1995). Gypsum is chosen because, in addition to behave same as a weak rock, is an ideal model material with which a wide range of brittle rocks can be represented (Nelson 1968); second, all the previous experiences and results can be incorporated and the earlier findings can be compared with the new ones; third, it allows to prepare a large number of specimens easily; Forth, repeatability of results. The samples are prepared from a mixture of the water and gypsum with a ratio of water to gypsum = 0. 75. Concurrent with the preparation of specimens and their testing, uniaxial compression and indirect tensile strengths of the intact material was also tested in order to control the variability of material. The uniaxial compressive strength (UCS) of the model material is measured on fabricated cylindrical specimens with 56 mm in diameter and 112 mm in length. The indirect tensile strength of the material is determined by the Brazilian test using fabricated solid discs 56 mm in diameter and 28 mm in thickness. The testing procedure of uniaxial compressive strength test and the Brazilian test complies with the ASTM D2938-86 (ASTM 1986) and ASTM C496-71 (ASTM 1971), codes respectively. Four transducers were used to measure the horizontal and vertical displacements in universal USC Tests. Three of the transducers are set to touch the middle of the cylindrical specimen longitudinally along a diametrical line at 120 degrees to each other while the other one is set to touch the base of the lower platen. The displacement transducers and load cell were connected to a data logger which was further linked to a PC for data recording. The base material properties derived from unconfined compression and tensile test are as follows
Average uniaxial compressive strength: 7.5 MPa
Average brazilian tensile strength: 4 MPa
Average Young's Modulus in compression: 10.5 GPa
Average Poisson's ratio: 0.18

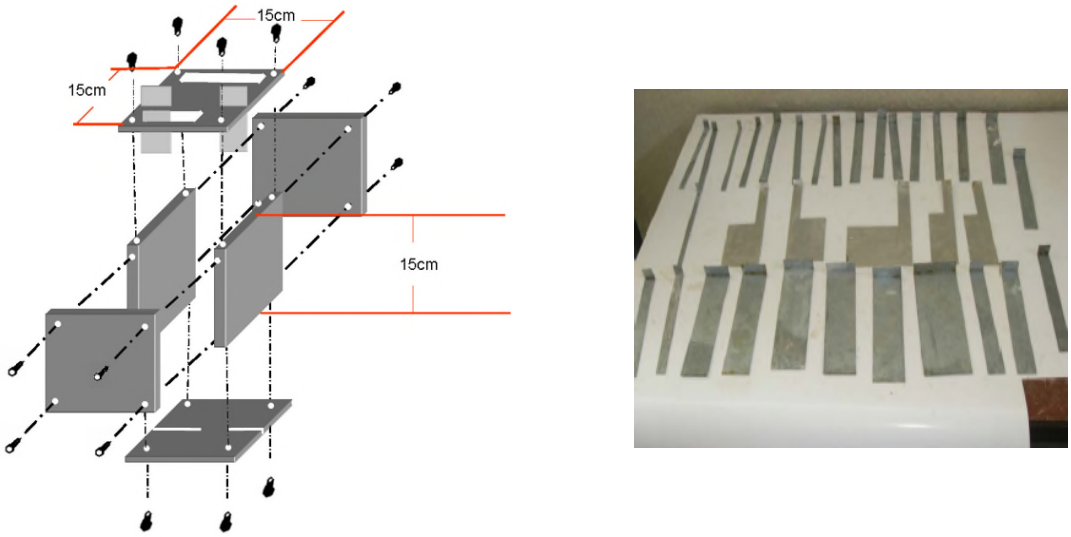

Fig. 2 Model used for the fabrication of the gypsum specimens

The technique in preparing the jointed specimens: Jointed specimens may be prepared by different methods that in general can be classified into two categories. The first involves inserting a medium between the two opposing surfaces that provides a lower friction angle in relation to the friction angle of the solid rock (Stimpson (1970). The second method entails assembling individual small blocks in a specific shape to form a large mass containing persistent or non-persistent joints (Brown and Trollope 1970, Rosenblad 1971, Ladanyi and Archambault 1981). The formation of jointed rock masses from individual block elements has the following shortcomings: Imperfect matching; Imperfect closure; imperfect matching or improper fitting of individual elements loads to concentration of stresses; Rotation; and Non-uniformity of the individual elements.

Due to the above-mentioned reasons (Bobet and Einstein 1998) developed a new method to form blocks with non-persistent joints during casting. The procedure developed by Bobet and Einstein (1998) for preparing open non-persistent joints was used in this research with some modifications. Following is a description of the procedure of making open coplanar non-persistent joints with different configurations. The material mixture is prepared by mixing water and gypsum in a blender; the mixture is then poured into a steel mold with internal dimension of 15×15×15 cm. The mold consist of four steel sheets, bolted together and of two PMMA plates 1cm thick, which are placed at the top and bottom of the mold, as shown in Fig. 2; the top plate has two rectangular openings used to fill the mold with the liquid gypsum mixture. The upper and the lower surfaces have slits cut into them. The opening of slits is 0.5 mm (0.02 inch) and their tract varies based on the width of the joints.

The positions and numbers of the slots are predetermined to give a desired non-persistent joint. Through these slits, greased metallic shims are inserted through the thickness of the mold before pouring the gypsum. The mold with the fresh gypsum is vibrated and then stored at room temperature for 8 h afterward, the specimens un-molded and the metallic shims pulled out of the specimens; the grease on the shims prevents adhesion with the gypsum and facilitates the removal of the shims.

As the gypsum seated and hardened, each shim leaves in the specimen an open joint through

Table 1(a) The geometrical specifications of the various rock bridges, (b) The Effective non-persistent joint Coefficients (EJC) for various configurations

Rock Bridge Set	R.B Area (cm^2)	a	b	c	d	e
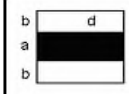	45	3	6	-	15	-
	90	6	4.5	-	15	-
	135	9	3	-	15	-
	45	3	6	-	15	-
	90	6	4.5	-	15	-
	135	9	3	-	15	-
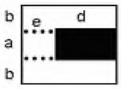	45	5	5	-	9	6
	90	9	3	-	10	5
	135	10	2.5	-	13.5	1.5
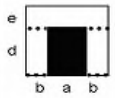	45	5	5	-	9	6
	90	9	3	-	10	5
	135	10	2.5	-	13.5	1.5
	45	1.5	4	4	15	-
	90	3	3	3	15	-
	135	4.5	2	2	15	-
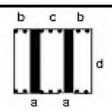	45	1.5	4	4	15	-
	90	3	3	3	15	-
	135	4.5	2	2	15	-
	45	2.5	4	2	9	6
	90	4.5	2	2	10	5
	135	5	2	1	13.5	1.5
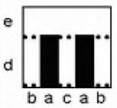	45	2.5	4	2	9	6
	90	4.5	2	2	10	5
	135	5	2	1	13.5	1.5
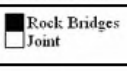						

(a)

Rock Bridge Set	Rock Bridge Arla (RB) cm^2	Effective Joint Surface (EJS) cm^2	Effective Joint Coefficients (EJC=EJS/(EJS+RB))
	45	0	0
	90	0	0
	135	0	0
	45	180	0.8
	90	135	0.6
	135	90	0.4
	45	30	0.4
	90	45	0.33
	135	15	0.1
	45	90	0.67
	90	60	0.4
	135	67.5	0.33
	45	0	0
	90	0	0
	135	0	0
	45	180	0.8
	90	135	0.6
	135	90	0.4
	45	0	0
	90	0	0
	135	0	0
	45	180	0.8
	90	135	0.6
	135	90	0.4
	45	30	0.4
	90	45	0.33
	135	15	0.1
	45	90	0.67
	90	60	0.4
	135	67.5	0.33

(b)

the thickness and perpendicular to the front and back of the specimen. Immediately after removing the shims, the front and back faces of the specimens are polished and the specimen is stored in laboratory for 4 days. At the end of the curing process, the specimens are tested. It does not appear that the pull out of the shims produces any damage to the flaws.

The planar rock bridges have various configurations respect to shear loading direction and have

occupied 45, 90 and 135 cm^2 of the total shear surface (225 cm^2) respectively. The geometry of non-persistent joints has shown in Table 1. Based on the change in the configuration and area of the rock-bridges, it is possible to define the Effective Joint Coefficient (EJC) as the ratio of the effective joint surface (EJS) that develops in front of the rock-bridge to the summation of the rock bridge surface and effective joint surface.

In Table 1(b), the effective joint surface that is in front of the rock bridges is shown as white area surrounded between the dotted lines. Furthermore, the amount of the EJC is exhibited in this table. These models were tested under normal stresses (σ_n) of 7.77 kg cm^{-2}.
Two identical specimens for each model are prepared and tested to check repeatability. If the results from two identical tests show significant differences, a third specimen is prepared and tested.

Testing equipment:

Testing of the specimens is done in direct shear until failure. These tests have been performed in an especially designed shear machine which complies with the requirements that were found to be indispensable in conventional shearing devices. Consequently, the shear boxes were provided with a high stiffness and with only one degree of freedom for the lower shear box in the horizontal direction and for the upper one in the vertical direction, corresponding to a shear displacement or dilation, respectively. Unwanted rotations and uncontrolled loading conditions could be prevented this way.

Testing program: A total of 48 direct shear tests have been performed. All tests are displacement-controlled. The tests were performed in such a way that the normal load was applied to the sample and then shear load was adopted. Readings of shear loads, as well as the shear displacements are taken every two seconds by a data acquisition system. Loading is carried out using displacement control at a rate of the 0.002 mm/s.
The failure mode, failure pattern and coalescence stress are the basic measurements

3. Observation

By observing the failure surface after the tests, it is possible to investigate the effect of rock bridge configurations (or EJC) on the failure pattern of specimens. Figs. 4-6 summarizes all observed crack patterns obtained in the direct shear tests. The crack pattern is always a combination of only two types of cracks: wing cracks and shear cracks.

Type I: The pure shear failure in persistent longitudinal rock bridges: The pure shear failure, as defined in Fig. 4, occurs when EJC=0; i.e. the persistent rock bridge have longitudinal configuration. In this case the shear bands initiated at the edges of the sample and developed to meet each other at a point in the bridge. Afterward the rock bridge gets broken into two parts from the middle with an uneven shear failure surface. The characteristics of the failure surface were investigated. There was a significant amount of pulverized and crushed gypsum and traces of shear displacement, indicated that a shearing failure had taken place. The shear failure mode appears in all types of samples consisting longitudinal rock-bridges (Fig. 4).

Type II: The oval mode coalescence with two wing cracks in persistent latitudinal rock bridges: The oval mode coalescence, as defined in Fig. 5(a) and 5(d), occurs when EJC=0.8; i.e. rock bridges have latitudinal configuration and theirs area is 45 cm^2. The wing cracks were

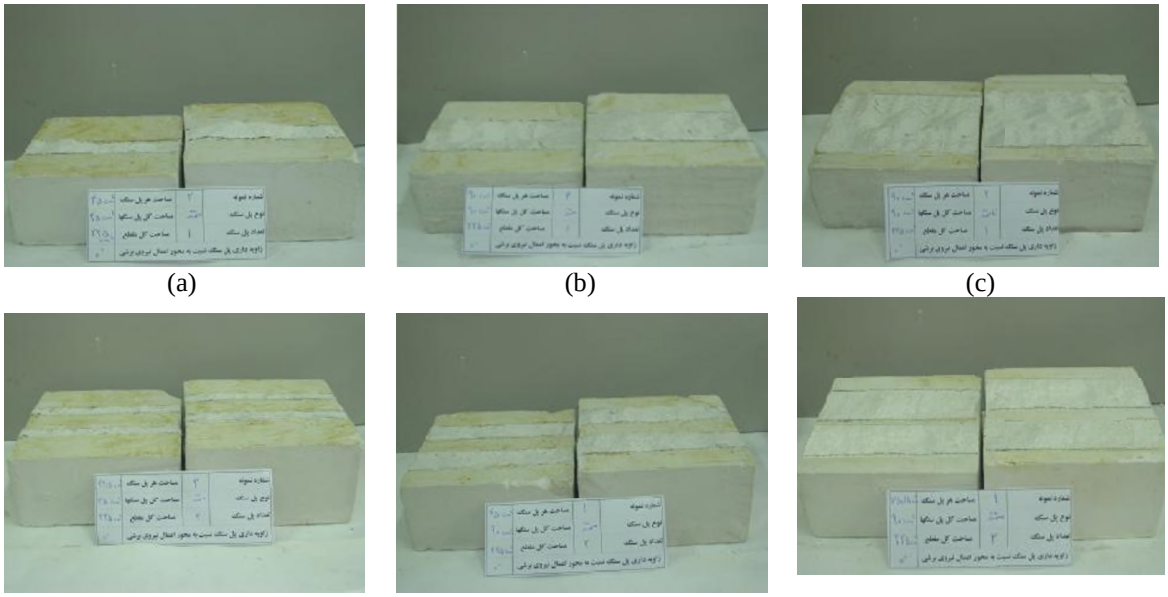

(a) (b) (c)

(d) (e) (f)

Fig. 4 The failure patterns in longitudinal rock bridges with EJC = 0

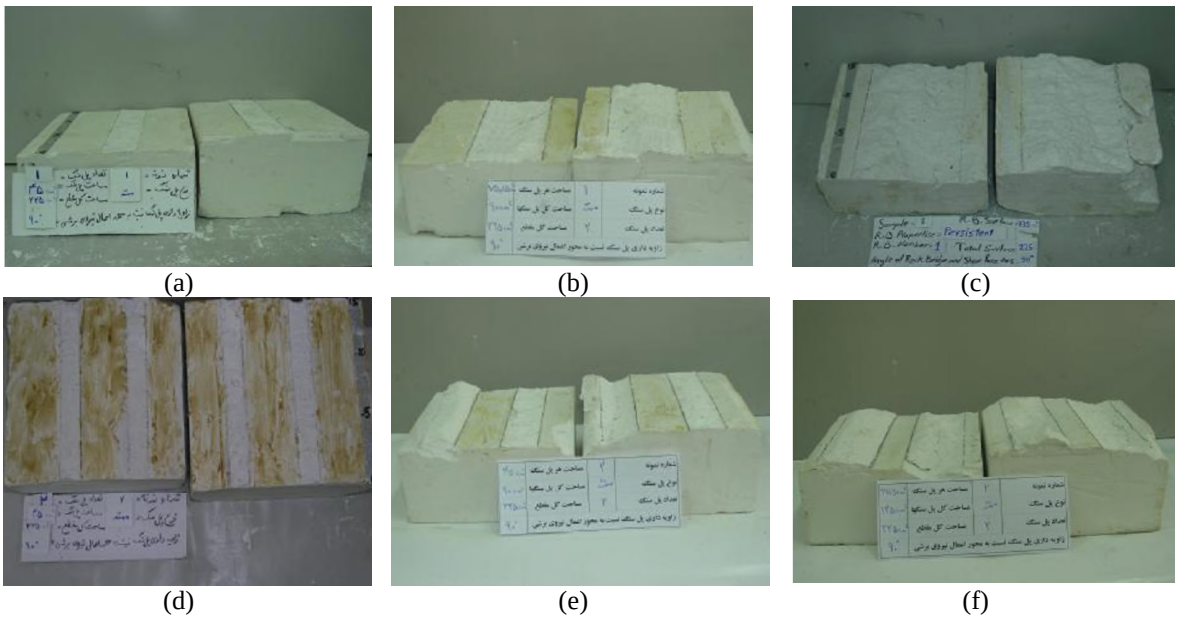

(a) (b) (c)

(d) (e) (f)

Fig. 5 The failure patterns in latitudinal rock bridge

initiated and propagated in curvilinear path that eventually aligned with the shear loading direction. The wing cracks propagate in a stable manner; and the external load needs to be increased for the cracks to propagate further. Each wing crack was initiated at the tip of one joint and finally coalesced with the tip of the other joint. This coalescence left an oval core of intact

material completely separated from the sample (Figs. 5(a) and 5(d)). The surface of failure at the bridge area is tensile because no crushed or pulverized materials and no evidence of shear movement were noticed. The wing cracks surfaces also had the same characteristics of tension surface. It is to be note that, when EJC=0.8 the oval mode coalescence appeared in samples consisting one and two latitudinal rock bridges.

Type III: Coalescence with one wing crack in persistent latitudinal rock bridges: This coalescence, as defined in Figs. 5(b) and 5(e), occurred when EJC=0.6; i.e. the persistent rock bridges have latitudinal configuration and theirs area is 90 cm^2. In this configuration the wing cracks were initiated at the tip of the joints and propagated stably. The upper tensile crack can propagate through the intact portion area and finally coalesced with the inner tip of the other joint but the lower tensile crack develops for a short distance and then become stable so as not to coalesce with the tip of opposite joint. Examining the wing crack surface it was noticed that there was smooth and clean with no crushed or pulverized material and no evidence of shear displacement. These surface characteristics indicated that tensile stresses were responsible for the initiation and propagation of the wing cracks. It is to be note that, when EJC=0.6 this coalescence appears in samples consisting one and two latitudinal rock bridges.

Type IV-Coalescence with two shear cracks in persistent latitudinal rock bridges: Coalescence with shear cracks, as defined in Figs. 5(c) and 5(f), occurs when EJC=0.4; i.e. the persistent rock bridges had latitudinal configuration and theirs area is 135 cm^2. The mechanism of failure was characterized first by initiation of wing cracks followed by the initiation of secondary cracks at the tips of the joint segments. Then the two wing cracks stopped while the two secondary cracks propagated to meet each other at a point in the bridge between the two inner tips of the pre-existing joints. The propagation and coalescence of the secondary cracks brought rock bridges to failure. The shear failure surface is in a wavy mode. Inspection of the surface of the cracks producing coalescence reveals the presence of many small kink steps, crushed gypsum and gypsum powder, which suggested coalescence through shearing. It is to be note that, when EJC=0.4, this coalescence appears in samples consisting one and two latitudinal rock bridges. As for the other experimental samples in this part, the failure patterns obtained from this experiment are in reasonable accordance with some of the related experimental results in Refs (Lajtai 1969, Zhang *et al*. 2006).

Type V: Coalescence with one undulating shear crack in non-persistent longitudinal rock bridges: This type of coalescence, as defined in Fig. 6, occurs when longitudinal rock bridges are non-persistent and EJC<0.4 (Figs. 6(a)-(f)). In this case, one wing crack was initiated at the inner tip of the joint and propagated stably in curvilinear path. Then the wing crack stopped while the secondary crack initiated at the inner tip of the joint and propagated stably to coalesce with the right edge of the sample, as shown in Fig. 6(a)-(f). It is to be noted that, when EJC < 0.4 this coalescence appeared in samples consisting one and two longitudinal non-persistent rock bridges.

Type VI: Coalescence with two shear cracks in latitudinal non-persistent rock bridges: This type of coalescence, as defined in Fig. 6, occurs when latitudinal rock bridges are non-persistent and EJC<0.4 (Figs. 6(g)-(l)). In this case, two wing cracks were initiated at the tips of the joints and propagated in curvilinear path. Then the two wing cracks stopped while the two secondary cracks initiated at the tips of the joint segments and continued to join together at a point in the bridge. It is to be note that, when EJC < 0.4 this coalescence appears in samples consisting one and two latitudinal non-persistent rock bridges. By examining the failure surface for non-persistent rock bridges, it was found that the shear failure surface is in a wavy mode. The traces of shear displacement existed and pulverized and crushed materials could be found. These surface

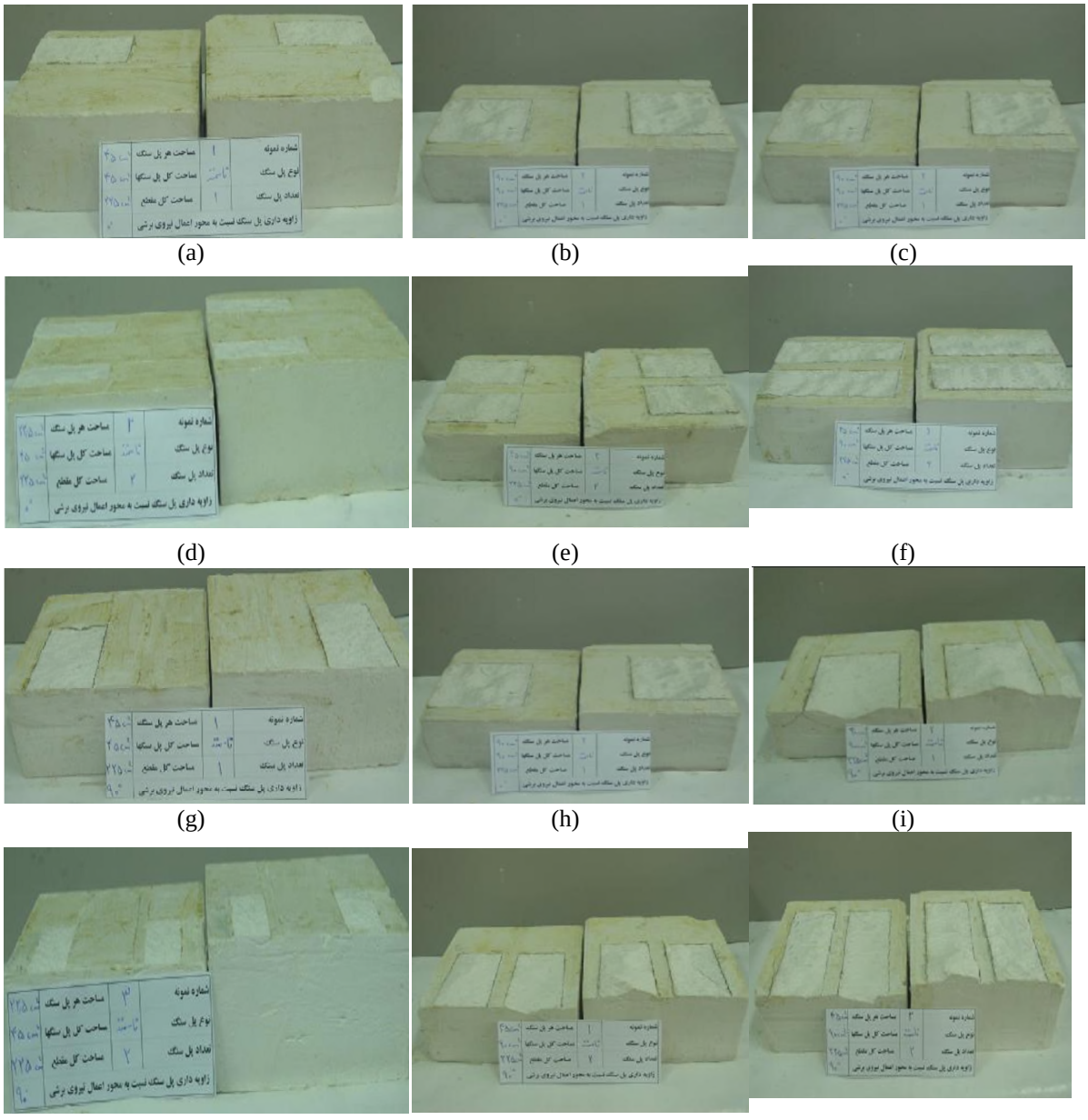

(a) (b) (c)

(d) (e) (f)

(g) (h) (i)

(j) (k) (l)

Fig. 6 The failure patterns in non-persistent rock bridges

characteristics indicated that shear stresses were responsible for the initiation of the shear cracks.

4. The effect of the effective joint coefficient (EJC) on the resistance of rock bridge

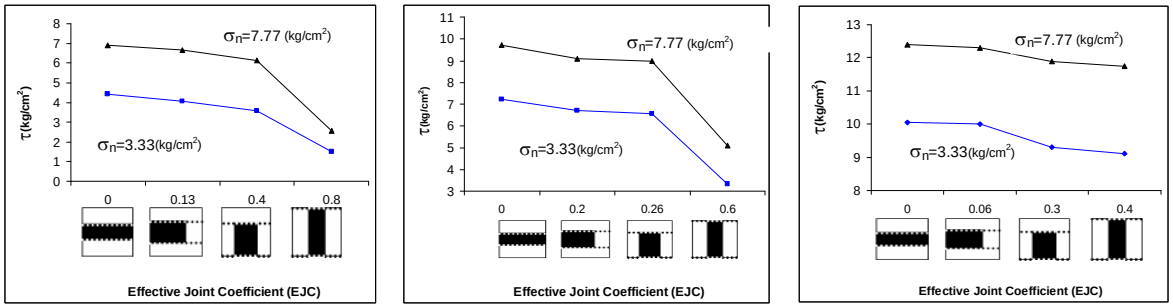

(a) (b) (c)

Fig. 7 Shear resistance versus effective joint coefficient (for one rock bridge); a: Area of the rock bridges is 45 cm^2, b: Area of the rock bridges is 90 cm^2, c: Area of the rock bridges is 135 cm^2

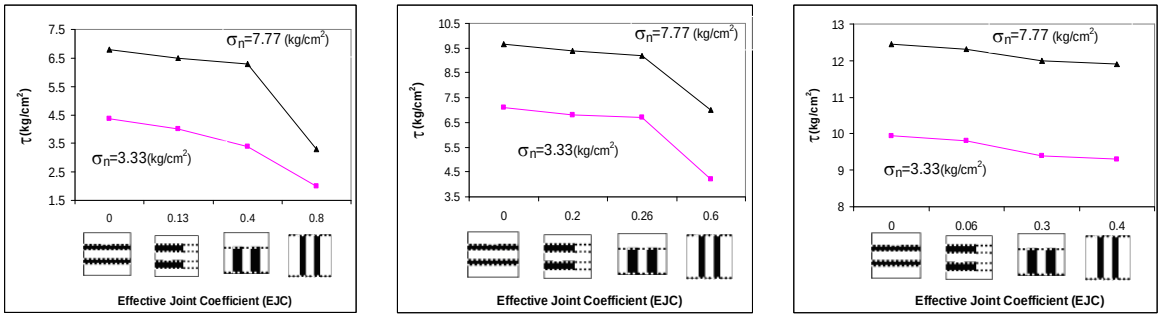

(a) (b) (c)

Fig. 8 Shear resistance versus effective joint coefficient (for two rock bridges); (a) Area of the rock bridges is 45 cm^2, (b) Area of the rock bridges is 90 cm^2, (c) Area of the rock bridges is 135 cm^2

Figs. 7 and 8 shows the rock-bridge resistance versus the EJC for one and two rock-bridges, respectively. Each figure summarizes the resistance at failure for three values of rock-bridge areas (45 cm^2, 90 cm^2 and 135 cm^2). the upper line and the lower line in Each panel represents the resistance of rock bridge under two value of the normal stress of 3.33 and 7.77 kg cm^{-2} respectively. From the Figs. 7 and 8, it can be found that for the fixed area of the rock bridge under fixed normal stress, the resistance decreases dramatically by increasing the EJC. The rock bridge resistance is maximum and minimum for longitudinal and latitudinal fully persistent rock bridge respectively. In fact, the coalescence stress depends on the EJC affecting the type of coalescence. When the rock-bridge extends longitudinally over the shear surface (EJC=0), there isn't any joint surface in front of the rock-bridge tips (Table 2(a) and (e)).

In this case, the stress concentration doesn't exist at the tip of the rock-bridge and the rock-bridge fails in its final resistance so has the maximum resistance. From the Fig. 7 and 8, it can be found that for the fixed area of the rock bridge under fixed normal stress, the resistance decreases dramatically by increasing the EJC. The rock bridge resistance is maximum and minimum for longitudinal and latitudinal fully persistent rock bridge respectively. In fact, the coalescence stress depends on the EJC affecting the type of coalescence. When the rock-bridge extends longitudinally over the shear surface (EJC=0), there isn't any joint surface in front of the rock-bridge tips. In this case, the stress concentration doesn't exist at the tip of the rock-bridge and the rock-bridge fails in its final resistance so has the maximum resistance. With the change in the configuration of the rock-bridge, the effective joint is formed in front of the rock-bridge, in such a way that in the latitudinal configuration of the rock-bridges, the value of EJC is maximum. The more be EJC, the higher be stress concentration at tips of the joints. So the smaller external loading need for reaching the stress concentration at tip of the joints to critical value. It means that the rock bridge resistance

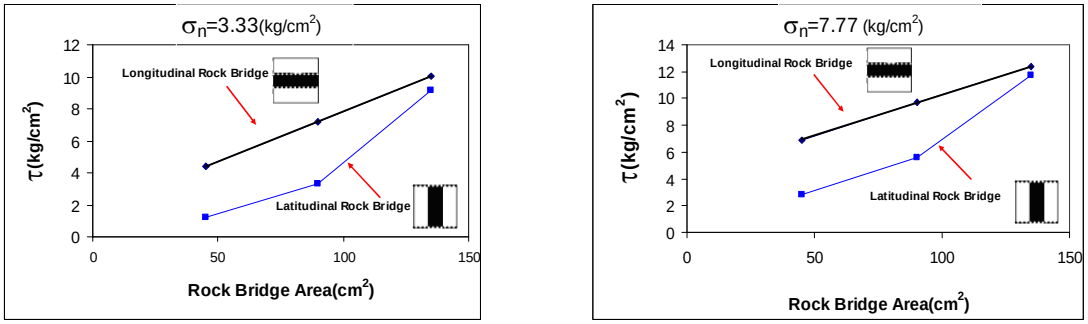

(a) (b)

Fig. 9 Shear resistance versus rock bridge area (for one latitudinal and longitudinal rock bridge); (a) The normal stress is 3.33 kg cm^{-2}, (b) The normal stress is 7.77 kg cm^{-2}

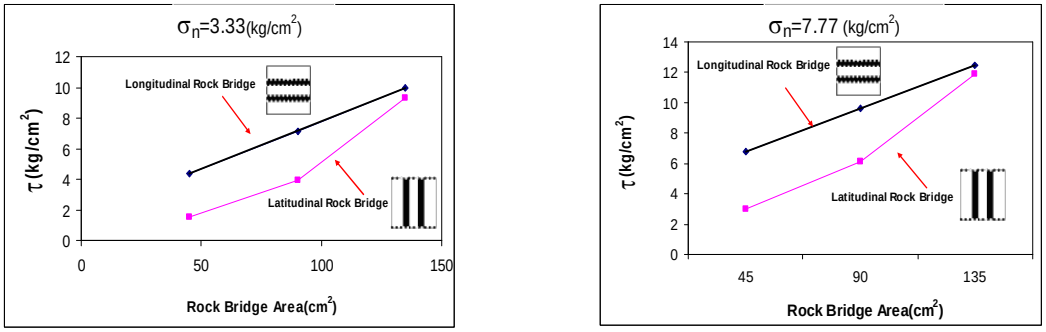

(a) (b)

Fig. 10 Shear resistance versus rock bridge area (for two latitudinal and longitudinal rock bridges); a: The normal stress is 3.33 kg cm^{-2}, b: The normal stress is 7.77 kg cm^{-2}

decreases by increasing the EJC. Since the longitudinal and latitudinal fully persistent rock-bridges have the minimum and maximum EJC, so their resistance behaviour will be inspected in following section.

5. Comparison of the latitudinal rock bridge resistance in the various areas of the rock bridge

Figs. 9 and 10 shows the rock-bridge resistance versus the area of one and two rock-bridges, respectively. Each figure summarizes the resistance at failure (τ_p) under two different values of normal stresses (σ_n) of 3.33 and 7.77 kg cm^{-2} respectively. The upper line and the lower line in each panel represent the resistance of longitudinal and latitudinal rock bridge respectively.

By comparing the resistance of the longitudinal and latitudinal rock-bridges in each figure, it is possible to reach the following conclusions.

1: In the fixed area of the rock bridge under fixed normal stress, the resistance of the latitudinal rock-bridges is less than the resistance of the longitudinal rock bridges (Figs. 9 and 10). Several aspects exist for this behaviour:

When the rock-bridge surface occupies 45 cm^2 of the total shear surface: In this condition the EJC is zero for longitudinal rock-bridges and the shear fracture occurred in rock segment (Figs. 4(a) and 4(d)) while for the latitudinal rock-bridges EJC is 0.8 and tensile fracture takes place in the rock-bridge (Figs. 5(a) and

5(d)). Since the tensile resistance of the rock bridge is less than its shear resistance, hence the smaller external load needs to bring the latitudinal rock bridge to tensile failure.

When rock-bridge surface occupies 90 cm^2 of the total shear surface: In this condition the EJC is zero for longitudinal rock-bridges and the shear fracture occurred in rock segment (Figs. 4(b) and 4(e)) while for the latitudinal rock-bridges EJC is 0.6 and tensile fracture takes place in the rock-bridge (Figs. 5(b) and 5(e)). So similar to former case the smaller external load needs to bring the latitudinal rock bridge to tensile failure.

When rock-bridge surface occupies 135 cm^2 of the total shear surface: In this condition, the shear fracture is occurred in both longitudinal and latitudinal rock-bridges ((Figs. 4(c) and 4(f)) and (Figs. 5(c) and 5(f)) but the shear resistance of the latitudinal rock-bridge is less than longitudinal rock bridges. This behaviour could be attributed to another effective facture. So that the EJC is zero for longitudinal rock-bridges but for the latitudinal rock-bridges EJC=0.4. The more be EJC, the higher be stress concentration at tips of the joints. It means that the shear resistance of the latitudinal rock-bridge is less than its amount in longitudinal rock bridges.

2: With reduction of the rock-bridge area under the fixed normal stress, the resistance reduction rate for the Latitudinal rock-bridge is more than longitudinal rock-bridges (Figs. 9 and 10). This has several reasons:

2-1: In longitudinal configuration of rock-bridges, the joint surface does not exist in front of the rock-bridge and the reduction in rock-bridge area is the only factor for the resistance reduction. But for the latitudinal configuration of rock bridges the joint surfaces are presented in front of the rock-bridge. With reduction of the rock bridge area, the joint surface is increased and the joint tips move closer to each other. Therefore a very high stress concentration (tensile and shear stress) is established at tip of the joints due to the interaction between the joint tips. These factors (i.e. the decreasing in rock bridge area and increasing in stress concentration) cause that the resistance reduction rate in the latitudinal rock-bridge be more than its amount in longitudinal rock-bridges.

2-2: With the reduction of the longitudinal rock-bridge area, the EJC=0 and the shear failure mode unchanged in the rock-bridge (Fig. 4). Therefore the shear resistance reduces at a linear rate. But for the latitudinal rock-bridge, with the reduction of the rock-bridge area, the EJC is increased and the shear failure mode changes to tensile failure (Fig. 5). Thus, the shear resistance reduces at a non-linear rate. It can be concluded from Fig, 9 and 10 that the EJC had significant effect on the resistance of rock bridge.

5. Determination of the slide direction in the rock slope with the presence of the coplanar non-persistent open discontinuity.

In the previous section, the effect of the effective joint Coefficient on the rock-bridge resistance is surveyed. In general, in the fixed area of the rock-bridge under fixed normal stress, the rock-bridge resistance is reduced with the increase of the Effective Joint Coefficient (EJC). With this experimental analysis, it is possible to determine the slide direction in the rock slopes containing coplanar non-persistent open discontinuity (Fig. 1). The openness of the joints and their engineering characteristics do not have any effect in the determination of the slide path. Also, it is assumed that the overburden weight W (normal stress) and the area of the rock-bridge have a same distribution in all of the possible slide paths and have no effect in the determination of slide path. In case, the effects of dynamic, water and asymmetrical forces are not considered, the configuration of the rock-bridges i.e. EJC lonely is the key factor in determination of the slide path. In this condition the slide takes place in the direction that EJC is maximum. Because, the more be the maximum effective joint Coefficient, the less be the sliding surface resistance.

6. Conclusions

The shear behaviour (failure progress, failure pattern, failure mechanism and shear resistance)

of rock specimens containing various configurations of rock bridges with different areas has been investigated under two different normal loads through direct shear test. The results show that the failure pattern is mostly influenced by EJC (the ratio of the surface of the joint that is in front of the rock-bridge and the total shear surface) while shear resistance is closely related to failure pattern and its mechanism. The following conclusions can be drawn from the experimental tests

1. In the fixed area of the rock-bridge under fixed normal stress, with the increase in the effective joint Coefficient, a very high stress concentration (tensile and shear stress) is established at tip of the joints due to the interaction between the joint tips.

2. With the increase in the effective joint Coefficient, the shear failure mode in the rock-bridge changes to the tensile failure mode.

3. The shear strength is closely related to the rock bridge failure pattern and failure mechanism, so that in the fixed area of the rock-bridge under fixed normal stress, the rock-bridge resistance reduced with change in failure mode from shear to tensile.

4. In the rock slopes containing coplanar non-persistent open discontinuity, assuming that the engineering characteristics of the joint, the overburden weight W (normal stress), the area of the rock-bridge, the dynamic, water and asymmetrical forces do not effect in the determination of the slide path, the slide will take place in the path which has the maximum amount of the effective joint coefficient. Because, the more be the maximum effective joint Coefficient, the less be the sliding surface resistance.

References

Akin M. (2013), "Slope stability problems and back analysis in heavily jointed rock mass: a case study from Manisa, Turkey", *Rock Mech. Rock Eng.*, **46(**2), 359-371.

ASTM (1971), "Standard method of test for splitting tensile resistance of cylindrical concrete specimens", ASTM designation C496-71.

ASTM (1986), "Test method for unconfined compressive resistance of intact rock core specimens", ASTM designation, 2938-86.

Bobet, A. and Einstein, H.H. (1998), "Fracture coalescence in rock-type materials under uniaxial and biaxial compression", *Int. J. Rock Mech. Min. Sci.*, **35**(7), 863-888.

Brown, E.T. and Trollop, D.H. (1970), "Resistance of a model of jointed rock", *J. Soil Mech. Found. Engrg, Proc.*, **96,** 685-704.

Duzgun, H.S.B. and Bhasin, R.K. (2009), "Probabilistic stability evaluation of Oppstadhornet rock slope", *Norway. Rock Mech. Rock Eng.*, **42**(5), 729-749.

Einstein, H.H., Veneziano, D., Baecher, G.B. and O'reilly, K.J. (1983), "The effect of discontinuity persistence on rock slope stability", *Int. J. Rock Mech. Min. Sci. Geomech. Abst.*, **20(**5), 227-236.

Gao,Y., Wu, D., Zhang, F., Lei, G.H., Qin, H. and Qiu, Y. (2016), "Limit analysis of 3D rock slope stability with non-linear failure criterion", *Geomech. Eng.*, **10**(1), 59-76.

Gehle, C. and Kutter, H.K. (2003), "Breakage and shear behaviour of intermittent rock joints", *Int. J. Rock Mech. Min. Sci.*, **40**(5), 687-700.

Ghazvinian, A., Nikudel, M.R. and Sarfarazi, V. (2007), "Effect of rock bridge continuity and area on shear behavior of joints", *Proceedings of the 11th Congress of the International Society for Rock Mechanics*, **1**, 247, CRC Press.

Gischig, V., Amann, F., Moore, J.R., Loew, S., Eisenbeiss, H. and Stempfhuber, W. (2011), "Composite rock slope kinematics at the current Randa instability, Switzerland, based on remote sensing and numerical modeling", *Eng. Geol.*, **118**(1), 37-53.

Grenon, M. and Hadjigeorgiou, J. (2008), "A design methodology for rock slopes susceptible to wedge

failure using fracture system modelling", *Eng. Geol.*, **96**(1), 78-93.
Haeri, H. (2015a), "Influence of the inclined edge notches on the shear-fracture behavior in edge-notched beam specimens", *Comput. Concrete*, **16**(4), 605-623.
Haeri, H. (2015b), "Experimental crack analyses of concrete-like CSCBD specimens using a higher order DDM", *Comput. Concrete*, **16**(6), 881-896.
Haeri, H. and Marji, M.F. (2016), "Simulating the crack propagation and cracks coalescence underneath TBM disc cutters", *Arab. J. Geosci.*, **9**(2), 1-10.
Haeri, H. and Sarfarazi, V. (2016), "The effect of micro pore on the characteristics of crack tip plastic zone in concrete", *Comput. Concrete*, **17**(1), 107-127.
Jaeger, J.C. (1971), "Friction of rocks and stability of rock slopes", *Geotech.*, **21**(2), 97-134.
Ladanyi, B. and Archambault, G. (1980), *Direct and indirect determination of shear resistance of rock mass*, AIME Annual Meeting, Las Vegas, 80-25.
Lajtai, E.Z. (1969), "Resistance of discontinuous rocks in direct shear", *Geotech.*, **19,** 218-233.
Li, D., Zhou, C., Lu, W. and Jiang, Q. (2009), "A system reliability approach for evaluating stability of rock wedges with correlated failure modes", *Comput. Geotech.*, **36**(8), 1298-1307.
Li, L.C., Tang, C.A., Zhu, W.C. and Liang, Z.Z. (2009), "Numerical analysis of slope stability based on the gravity increase method", *Comput. Geotech.*, **36**(7), 1246-1258.
Li, Y.P., Chen, L.Z. and Wang, Y.H. (2005), "Experimental research on pre-Cracked marble", *Int. J. Solid. Struct.*, **42,** 2505-2016.
Momber, A.W. and Kovacevic, R. (1997), "Test parameter analysis in abrasive water jet cutting of rocklike materials", *Int. J. Rock Mech. Min. Sci.*, **34**(1), 17-25.
Mughieda, O. and Alzo'ubi, A.K. (2004), "Fracture mechanisms of offset rock joints-A laboratory investigation", *Geotech. Geol. Eng.*, **22**(4), 545-562.
Mughieda, O. and Karasneh, I. (2006), "Coalescence of offset rock joints under biaxial loading", *Geotech. Geol. Eng.*, **24**(4), 985-999.
Mughieda, O.S. and Khawaldeh, I. (2004), "Scale effect on engineering properties of open non-persistent rock joints under uniaxial loading", *Proceedings of the 7th Regional Rock Mechanics Symposium*, Sivas, Türkiye.
Naghadehi, M.Z., Jimenez, R., KhaloKakaie, R. and Jalali, S.M.E. (2011), "A probabilistic systems methodology to analyze the importance of factors affecting the stability of rock slopes", *Eng. Geol.*, **118**(3), 82-92.
Nelson, R. (1968), "Modeling a jointed rock mass", MS Thesis, Mass. Inst. Tech., Cambridge.
Nelson, R.A. and Hirschfeld, R.C. (1968), "Modeling a jointed rock mass", Report R68-70, Mass. Inst. Tech., Cambridge.
Pantelidis, L. (2011), "A critical review of highway slope instability risk assessment systems", *B. Eng. Geol. Envir.*, **70**(3), 395-400.
Regmi AD, Yoshida K, Nagata H *et al*, 2013 The relationship between geology and rock weathering on the rock instability along Mugling–Narayanghat road corridor, Central Nepal Himalaya. Nat Hazards 66:501–532.
Regmi, A.D., Yoshida, K., Nagata, H., Pradhan, A.M.S., Pradhan, B. and Pourghasemi, H.R. (2013), "The relationship between geology and rock weathering on the rock instability along Mugling-Narayanghat road corridor, Central Nepal Himalaya", *Nat. Hazards*, **66**(2), 501-532.
Reyes, O. and Einstein, H.H. (1991), "Failure mechanisms of fractured rock-a fracture coalescence model", *Proceedings of the 7th ISRM Congress, Int. Soc. Rock Mech*.
Robertson, A.M. (1970), "The interpretation of geological factors for use in slope theory", *Proceedings of the Planning Open Pit Mines*, Johannesburg.
Rosenblade, J.L. (1971), "Geomechanical model study of the failure modes of jointed rock masses", Ph.D Thesis, University of Illinois at Urbana-Champaign, Il, USA.
Sharma, R.K., Mehta, B.S. and Jamwal, C.S. (2013), "Cut slope stability evaluation of NH-21 along Nalayan-Gambhrola section, Bilaspur district, Himachal Pradesh, India", *Nat. Hazards*, **66**(2), 249-270.
Shen, B., Stephansson, O., Einstein, H.H. and Ghahreman, B. (1995), "Coalescence of fractures under shear

stresses in experiments", *J. Geophy. Res.*, **100**(6), 5975-5990.
Shen, B., Stephansson, O., Einstein, H.H. and Ghahreman, B. (1996), "Coalescence of fractures under shear stress experiments", *J. Geophys. Res.*, **6**, 5975-5990.
Singh, T.N., Gulati, A., Dontha, L. and Bhardwaj, V. (2008), "Evaluating cut slope failure by numerical analysis-a case study", *Nat. Hazards*, **47**(2), 263-279.
Stimpson, B. (1970), "Modelling materials for engineering rock mechanics", *Int. J. Rock Mech. Min. Sci. Geomech. Abst.*, **7**(1), 77-121, Pergamon.
Taheri, A. and Tani, K. (2010), "Assessment of the stability of rock slopes by the slope stability rating classification system", *Rock Mech. Rock Eng.*, **43**(3), 321-333.
Takeuchi, K. (1991), "Mixed-mode fracture initiation in granular brittle materials", M.S. Thesis, Mass. Inst. Tech., Cambridge.
Terzaghi, K. (1962), "Stability of steep slopes on hard unweathered rock", *Geotech.*, **12**(4), 251-270.
Zhang, H.Q., Zhao, Z.Y., Tang, C.A. and Song, L. (2006), "Numerical study of shear behavior of intermittent rock joints with different geometrical parameters", *Int. J. Rock Mech. Min. Sci.*, **43**(5), 802-816.
Zhao, L.H., Cao, J., Zhang, Y. and Luo, Q. (2015), "Effect of hydraulic distribution on the stability of a plane slide rock slope under the nonlinear Barton-Bandis failure criterion", *Geomech. Eng.*, **8**(3), 391-414.

CC